Density Functional Study of Chemical Stability and Nitrogen Encapsulation of $C_{48}N_{12}$ and $C_{58}N_{12}$

Jin Qiang Hou[†] and Hong Seok Kang*

Department of Nano and Advanced Materials, College of Engineering, Jeonju Univesity, Hyoja-dong, Wansan-Ku, Chonju, Chonbuk 560-759, Republic of Korea

Received: May 10, 2006; In Final Form: August 29, 2006

On the basis of calculations using density functional theory, we show that $C_{58}N_{12}$, just as $C_{48}N_{12}$, can be a stable N-dopant of C_{70}. By considering many different isomers of the product, we find that the chemical stability of $C_{48}N_{12}$ and $C_{58}N_{12}$, with respect to oxygenation, is not significantly different from that of C_{70}, thereby indicating that the N-dopant would not easily be oxygenated in air under normal conditions. In both $C_{48}N_{12}O$ and $C_{58}N_{12}O$, many different isomers are expected, in which oxygenation occurs at different C−N bonds as well as at C−C bonds, among which specific C−N bonds are the most amenable to the reaction. Investigation of their hydrogenations shows that $C_{48}N_{12}$ is slightly more easily hydrogenated than C_{60}, while $C_{58}N_{12}$ is less easily hydrogenated. In addition, we expect a regiospecificity in the hydrogenated products of $C_{58}N_{12}$, which prefers to react at equatorial sites, while C_{70} prefers reaction at polar sites. Meanwhile, comparison of the encapsulation energy of a nitrogen atom (=N_{en}) in C_{60}, $C_{48}N_{12}$, C_{70}, and $C_{58}N_{12}$ shows that the N-doped fullerenes, particularly $C_{58}N_{12}$, can encase the atom much better than the undoped ones, allowing us to expect the existence of $N@C_{48}N_{12}$ and $N@C_{58}N_{12}$. Spin multiplicities are doublet for most of their stable structures. These observations correlate with the formation of N_{en}−C bonds, which are not found in $N@C_{60}$ and $N@C_{70}$. Various isomers of the N-encapsulating fullerenes were identified. The relative stability of these isomers heavily depends on the number of substitutional nitrogen atoms around N_{en}−C bonds.

1. Introduction

Since the discovery of $C_{59}N$,[1] azafullerenes have been considered as new materials which can be used for designing materials in a solid state. Particularly, a new fullerene-like material was recently reported which consists of cross-linked nano-onions of C and N from a magnetic sputtering of graphite in N_2.[2] Using an electron microscope and energy loss spectroscopy, in conjunction with calculations based on the density functional theory (DFT), shows that the core of concentric fullerene-like shells corresponds to $C_{48}N_{12}$, a substitutional N-dopant of C_{60}. Nano-indentation tests detected highly elastic properties of the material, rendering it ideal for wear-protective materials. It was also shown to be a promising component of a molecular rectifier.[3] This leads us to investigate the possibility of the existence of a similar N-dopant derived from C_{70}. On the basis of a DFT calculation, we will show that $C_{58}N_{12}$ can indeed be such a derivative.

A DFT calculation shows that the most stable structure (=S_6 symmetry) of $C_{48}N_{12}$ has two triphenylene-type units in the polar region and six nitrogen atoms in the equatorial region.[4] Nitrogen atoms are distributed in such a pattern in which each pentagon has only one nitrogen atom. Electronic, Raman, and IR studies on a low-lying isomer were also reported. [5−8] In addition, the electronic structure of solid $C_{48}N_{12}$ was investigated;[9] however, the chemical stability of the N-dopant has never been studied. It deserves attention, since chemical stability is the basic requirement for its use in nanoelectronic devices. Its stability with respect to oxygenation in the air is of particular interest for such a purpose. This work is devoted to the study of that problem using the DFT method. We will also evaluate its relative ease of hydrogenation, compared with that of C_{60}. A similar investigation will be done for $C_{58}N_{12}$ in comparison with the stability of C_{70}. Finally, we will also investigate the possible formation of endohedral fullerenes $N@C_{48}N_{12}$ and $N@C_{58}N_{12}$. This study will be conducted because $N@C_{60}$ was known to exist, where the fullerene acts as a Faraday cage which can shield the interior of the cage from an unwanted external electric field.[10]

2. Theoretical Method

Our total energy calculations are performed by using the Vienna ab initio simulation package (VASP).[11] Electron−ion interaction is described by the projected augmented wave (PAW) method,[12] which is basically a frozen-core all-electron calculation. The exchange-correlation effect is treated within the generalized gradient approximation presented by Perdew, Burke, and Ernzerhof (PBE).[13] The solution of the Kohn−Sham (KS) equation is obtained by using the Davison blocked iteration scheme followed by the residual vector minimization method. All valence electrons of the chemical elements are explicitly considered in the KS equation. We adopt a supercell geometry for which *k*-space sampling is done with Γ-point. In doing this, we use large supercells which ensure the interatomic distance between neighboring cells greater than 7.00 Å. The cutoff energy is set high (=400 eV) enough to guarantee accurate results, and the conjugate gradient method is employed to optimize its geometry until the Hellmann−Feynman force exerted on an atom is less than 0.03 eV/Å. Reliability of the PBE calculation within the PAW was confirmed by recent calculations on the

* To whom correspondence should be addressed. E-mail: hsk@jj.ac.kr.
[†] Permanent address: Pohl Insitute of Solid State Physics, Tongji University, Shanghai 200092, People's Republic of China.

10.1021/jp0628535 CCC: $33.50
Published on Web 10/17/2006

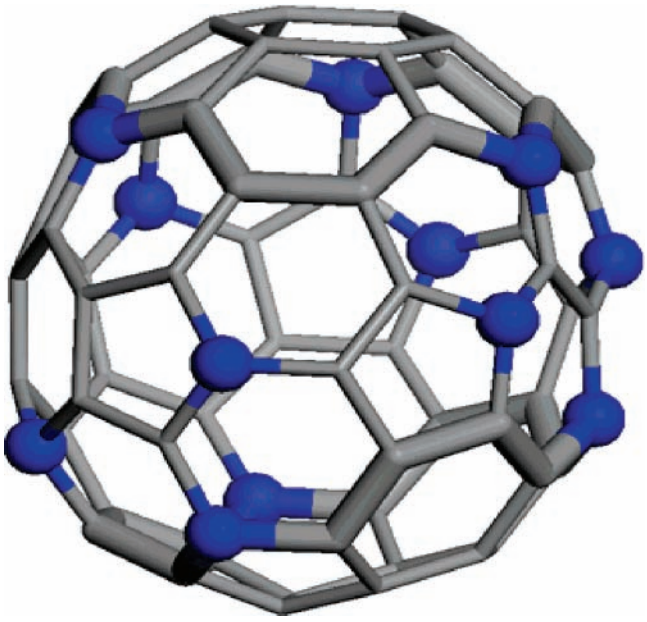

Figure 1. Optimized structure of $C_{58}N_{12}$. Polar regions are defined by the triphenylene-type local structures and are surrounded by thick bonds. Nitrogen atoms are represented by balls.

electronic and chemical properties of metal−aromatic sandwich complexes to nanotubes.[14]

3. Results

Here, we briefly describe the nitrogen substitution on C_{70}. In $C_{58}N_{12}$, half of the 12 nitrogen atoms are assumed to be located in the polar region (i.e., in two triphenylene units) in a way similar to those in $C_{48}N_{12}$, while the other half are located in the equatorial region. (See Figure 1.) This distribution complies with the idea that every five-membered ring has one nitrogen atom. In $C_{60}N_{10}$, when compared to $C_{58}N_{12}$, there are two fewer nitrogen atoms in its equatorial region. Three isomers were considered. Our structure optimization shows that their relative energies lie within 0.69 eV of each other. For $C_{62}N_8$, we have considered two isomers, which still have two fewer nitrogen atoms in the equatorial region. Relative energies of the optimized structures of the two isomers lie within 0.1 eV. For $C_{56}N_{14}$, four different isomers were considered. In each of them, two additional nitrogen atoms other than those in $C_{58}N_{12}$ were located in the equatorial region. Our structure optimization shows that their relative energies lie within 0.53 eV of each other. Using the lowest energy structure for each of $C_{70-n}N_n$, we have calculated the energy differences using the following equation, $\Delta E(n) = E[C_{70-n}N_n] - E[C_{72-n}N_{n-2}]$ as a function of n. We find that it is nearly a constant (~2.6 eV) up to $n = 12$, but it abruptly increases to 4.2 eV at $n = 14$. This behavior is similar to $C_{48}N_{12}$,[2] showing that the maximum number of substitutional nitrogen atoms in $C_{70-n}N_n$ is also 12.

A comparison of the electronic structures of N-doped systems with those of an undoped nature also shows interesting results. Comparing the HOMO−LUMO gaps of C_{70} (=1.71 eV) and $C_{58}N_{12}$ (=0.75 eV) shows that the gap decreases by a significant amount (=0.96 eV) upon the substitutional introduction of 12 nitrogen atoms in the latter. This correlates with the observation that LUMO of $C_{58}N_{12}$ is characterized by the electron density pronounced on nitrogen atoms, while it is not the case in HOMO. This distribution stabilizes the LUMO level with respect to the HOMO level, since nitrogen atoms are more electronegative than carbon atoms. Overall, 10 out of 12 nitrogen atoms were found to hold an appreciable amount of electron density in LUMO, while only 6 have a similar amount in HOMO. This is different from the case of $C_{48}N_{12}$, in which there is an appreciable amount of electron density on 12 nitrogen atoms in both HOMO and LUMO. As a result, the HOMO−LUMO gap is smaller than that (=1.36 eV) of $C_{48}N_{12}$ obtained from our calculation. The latter gap is highly close to the band gap (=1.3 eV) of $C_{48}N_{12}$ calculated at the PW91 level.[9]

TABLE 1: Energy of Oxygenation (ΔE_{oxy}) and Bond Lengths in $C_{60}O$ and $C_{48}N_{12}O$[a]

isomer	ΔE_{oxy} (eV)	l_1 (Å)	l_2 (Å)	l_3 (Å)
$C_{60}O$ D_{6C-6C}	−4.11	1.43	1.43	1.54 (1.40)
$C_{60}O$ D_{5C-6C}	−4.08	1.39	1.39	2.15 (1.45)
$C_{48}N_{12}O$ E_{5C-6N}	−4.99	1.23	2.72	2.03 (1.42)
$C_{48}N_{12}O$ E_{5C-6C}	−4.70	1.44	1.47	1.47 (1.37)
$C_{48}N_{12}O$ E_{6C-6N}	−4.31	1.28	2.46	1.61 (1.42)
$C_{48}N_{12}O$ B_{5C-6N}	−4.00	1.24	2.79	2.12 (1.44)
$C_{48}N_{12}O$ B_{6C-6C}	−3.87	1.42	1.46	1.52 (1.40)
$C_{48}N_{12}O$ P_{6C-6C}	−3.65	1.42	1.42	1.64 (1.43)

[a] l_1, l_2 denote the bond lengths of C−O or N−O bonds, and l_3 is that of C−C or C−N bond. Isomers of $C_{48}N_{12}O$ are defined in Figures 2 and S1 (Supporting Information). The numbers in parentheses denote the bond lengths of the corresponding C−C or C−N bonds in C_{60} and $C_{48}N_{12}$.

Next, we describe the oxygenation of N-doped fullerenes in comparison with that of undoped ones in order to estimate the chemical stability of the former in the air. In many C_{60} syntheses, $C_{60}O$ is generated as a minor component.[15] In C_{60}, a typical oxygenation occurs at a [6,6] bond through the photooxygenation of the molecule by irradiating an oxygenated benzene solution, resulting in the 1,2-bridged epoxyfullerene, $C_{60}O$.[16] The epoxide is also formed by allowing the toluene solution of C_{60} to react with dimethyldioxirane.[17] Oxidation at a [5,6] bond is also found to result from the photolysis of $C_{60}O_3$.[18] Here, we make a systematic investigation of the oxidation of N-doped fullerenes in comparison with that of undoped ones. In consistency with a previous report,[19,20] we find that the oxidation of C_{60} is energetically more favorable at a [6,6] bond than at a [5,6] bond by a marginal amount (=0.02 eV). See isomers D_{6C-6C} and D_{5C-6C} in Table 1, respectively. In agreement with spectroscopic analysis,[16] our energy minimization shows that oxygenation at a [6,6] bond results in the elongation of the bond to a single bond (=1.54 Å). Meanwhile, Table 1 shows that the reaction at a [5,6] bond results in a breaking of the bond.[20]

In the study of the oxidation of $C_{48}N_{12}$, we considered six isomers. Each of them is distinguished from one another by the fact that the reaction occurs at a different C−C or C−N bond. As shown in Figure 2a, the most stable isomer (=E_{5C-6N}) corresponds to oxygenation at a [5,6] C_1-N_2 bond in the equatorial region (=E). According to Table 1, its energy of oxidation, ΔE_{oxy} (=−4.99 eV), defined by the process $C_{48}N_{12} + O \rightarrow C_{48}N_{12}O$, shows that the oxidation is more favorable than that of C_{60} by 0.88 eV, thus revealing the ease of oxidation of $C_{48}N_{12}$. The C_1-N_2 bond becomes broken. Instead, a carbonyl bond is formed involving the carbon atom released (=C_1), which can be seen in the $C_1=O_3$ bond length (=1.23 Å), which corresponds to a double bond. [21] The nitrogen atom released (=N_2) remains bonded to only two carbon atoms. The oxygen atom (=O_3) does not lie on the plane defined by the sp^2 hybridization of the carbonyl carbon (=C_1). This is presumably because that configuration reduces the repulsion between O_3 and the lone pair electrons of N_2. Figure 2b shows the next stable isomer (=E_{5C-6C}), which is energetically comparable to the most stable one. In the isomer, there is an epoxidation at one of the [5,6] C−C bonds in the equatorial region. The C−C

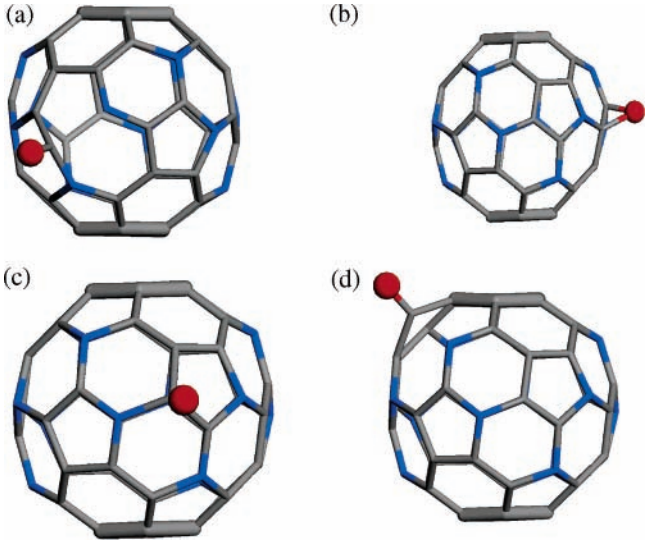

Figure 2. Optimized structures of isomers of $C_{48}N_{12}O$: E_{5C-6N} (a), E_{5C-6C} (b), E_{6C-6N} (c), and B_{5C-6N} (d). Labels E, P, and B denote that the reaction occurs at the equatorial, polar regions, and the boundary of two regions. Hexagons in the polar regions are surrounded by thick bonds.

bond involved in oxidation becomes elongated by 0.10 Å. The next stable isomer (=E_{6C-6N}) shown in Figure 2c is characterized by oxygenation at a [6,6] C_1-N_2 bond in the equatorial region. Another isomer, B_{5C-6N} shown in Figure 2d, is slightly less stable, being also characterized by the breaking of a C−N bond and the formation of a C=O bond. According to our convention, two other isomers shown in Figure S1a and S1b (Supporting Information) can be denoted by B_{6C-6C} and P_{6C-6C}. Here, the letter "B" indicates that oxygenation occurs at the boundary of polar and equatorial regions, and the letter "P" denotes that the bond is formed in the polar region. In short, the presence of C−N bonds in $C_{48}N_{12}$ brings about diversity in the oxidation products. C−N bonds are generally more amenable to oxygenation than C−C bonds, implying that $C_{48}N_{12}$ can be more easily oxygenated than C_{60}.

Next, we consider the oxygenation of C_{70} and its N-dopants. To do this, we need to calculate ΔE_{oxy}. Five isomers of $C_{70}O$ were considered**.** In agreement with previous calculations,[22] the most stable isomer in Figure 3a, denoted by E_{6C-6C} in Table 2, has a C−O−C bond which replaces a [6,6] C−C bond, where the C−C bond taking part in the oxygenation becomes broken upon oxygenation. [See the C−C distance (=2.17 Å) in the table.] Its value of $E_{oxy}(C_{70})$ (=−4.48 eV) shown in Table 2 indicates that its formation is not appreciably more favorable than that of $C_{60}O$, indicating that the stability of C_{70} with respect to oxygenation is similar to that of C_{60}. In consistency with this observation, Diedrich and co-workers were able to identify $C_{70}O$ from the resistive heating of graphite, not under normal synthetic conditions for C_{70} at room temperature.[23] Nor, it is produced under the exposure of C_{70} to air.[23] According to the table, the stabilities of four other isomers shown in Figure 3b−e are similar to each other. They are P_{6C-6C}, P_{5C-6C}, E_{5C-6C}, and B_{6C-6C}, whose ΔE_{oxy} are also comparable to that of the isomer E_{6C-6C}. Therefore, the oxidation product of C_{70} will be a mixture of all five isomers. In accordance with these results, many different isomers of $C_{70}O$ were identified in the ozonization of the C_{70} solution.[24]

Now, we describe the oxidation of $C_{58}N_{12}$. Nine different isomers were considered, as shown in Figures 4 and S2 (Supporting Information) and Table 3. Similar to the case of $C_{48}N_{12}$, the most stable isomer [=B_{5C-6N} in Figure 4a] corresponds to the oxygenation at the [5,6] C−N bond; however, the C−N bond is not located in the equatorial region but at the boundary (=B) of the polar and equatorial regions. The comparison of its oxygenation energy with that of C_{70} indicates that the chemical stability of $C_{58}N_{12}$, with respect to oxygenation in air, is similar to that of C_{70}. We also find that $C_{58}N_{12}$ is less easily subject to oxidation than $C_{48}N_{12}$. Again, we expect a diversity in its possible isomers in which oxygenations occur at both equatorial and polar sites. [See Figures 4 and S2 (Supporting Information).]

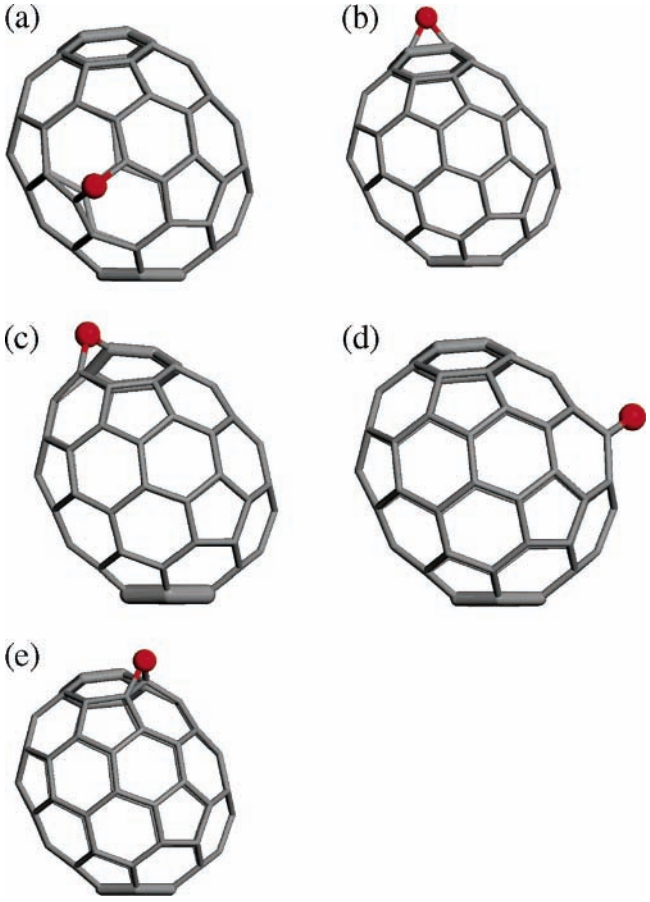

Figure 3. Optimized structures for isomers of $C_{70}O$: E_{6C-6C} (a), P_{6C-6C} (b), P_{5C-6C} (c), E_{5C-6C} (d), and B_{6C-6C} (e). Also refer to the caption of Figure 2.

TABLE 2: Energy of Oxygenation (ΔE_{oxy}) and Bond Lengths in $C_{70}O$[a]

isomer	ΔE_{oxy} (eV)	l_1 (Å)	l_2 (Å)	l_3 (Å)
E_{6C-6C}	−4.48	1.39	1.40	2.17 (1.47)
P_{6C-6C}	−4.06	1.43	1.43	1.55 (1.40)
P_{5C-6C}	−4.05	1.39	1.39	2.13 (1.45)
E_{5C-6C}	−4.04	1.40	1.40	2.11 (1.44)
B_{6C-6C}	−4.01	1.43	1.43	1.54 (1.39)

[a] Isomers of $C_{70}O$ are defined in Figure 3. The numbers in parentheses denote the bond lengths of the corresponding C−C bonds in C_{70}. See also footnote *a* for Table 1.

We are also interested in the relative ease of the hydrogenation of the fullerenes in the process, fullerene + H_2 → fullerene-H_2. In accordance with PM3 calculations,[25] Table 4 and Figure 5a show that the most stable isomer (=isomer A) of $C_{60}H_2$ has a 1,2-hydrogenation at the [6,6] bond. Its energy of hydrogenation is −0.87 eV. The table and Figure 5b show that the next most stable isomer (=isomer B) is characterized by 1,4-hydrogenation, which is energetically higher than isomer A by 0.30 eV. This is different from the PM3 calculation, which

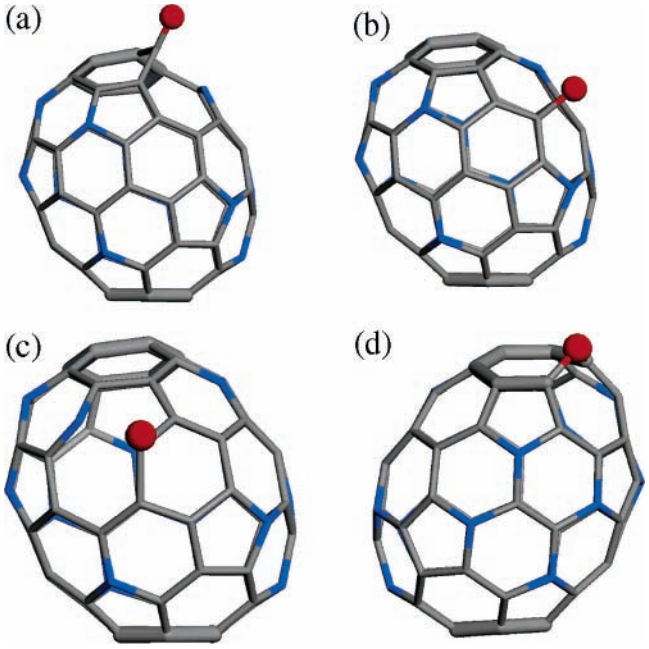

Figure 4. Optimized structures for isomers of $C_{58}N_{12}O$: B_{5C-6N} (a), E_{6C-6C} (b), E_{5C-6N} (c), and P_{6C-6C} (d). Also refer to the caption of Figure 2.

TABLE 3: Energy of Oxygenation (ΔE_{oxy}) and Bond Lengths in $C_{58}N_{12}O$[a]

isomer	ΔE_{oxy} (eV)	l_1 (Å)	l_2 (Å)	l_3 (Å)
B_{5C-6N}	−4.37	1.23	2.82	2.17 (1.41)
E_{6C-6C}	−4.26	1.43	1.49	1.53 (1.43)
E_{5C-6N}	−4.16	1.25	2.68	1.97 (1.42)
P_{6C-6C}	−4.04	1.38	1.38	2.16 (1.43)
E_{5C-6C}	−3.85	1.43	1.49	1.51 (1.42)
E_{6C-6C}	−3.79	1.48	1.45	1.50 (1.42)
P_{5C-6C}	−3.64	1.46	1.46	1.54 (1.43)
E_{6C-6C}	−3.27	1.46	1.43	1.57 (1.43)
E_{6C-6N}	−2.76	1.37	1.40	2.22 (1.42)

[a] Isomers of $C_{58}N_{12}O$ are defined in Figures 4 and S2 (Supporting Information). The numbers in parentheses denote the bond length of the corresponding C−C or C−N bonds in $C_{58}N_{12}$. Also refer to footnote *a* of Table 1.

TABLE 4: Energy of Hydrogenation (ΔE) at the Different Positions of C_{60}, $C_{48}N_{12}$, C_{70}, and $C_{58}N_{12}$[a]

	isomer	ΔE (eV)		isomer	ΔE (eV)
$C_{60}H_2$	A	−0.87	$C_{70}H_2$	E_{6C-6C}^{δ}	−0.14
	B	−0.57		E_{6C-6C}^{η}	0.72
	C	−0.09	$C_{58}N_{12}H_2$	E_{5C-6C}^{ζ}	−0.60
$C_{48}N_{12}H_2$	E_{5C-6C}	−1.55		E_{6C-6C}^{δ}	−0.14
	P_{6C-6C}	−0.13		P_{6C-6C}^{α}	0.03
	B_{5C-6N}	0.35		E_{5C-6N}^{ζ}	0.05
	E_{5C-6N}^{ζ}	0.54		P_{6C-6C}^{β}	0.13
	E_{6C-6N}	0.85		B_{5C-6N}^{ζ}	0.56
$C_{70}H_2$	P_{6C-6C}^{α}	−0.84		E_{6C-6N}^{δ}	0.77
	P_{6C-6C}^{β}	−0.69			

[a] Resulting isomers are defined in Figures 5−7, 9, and S3 (Supporting Information).

showed that its energy is the same as that of isomer A.[25] Another isomer (=isomer C), described by hydrogenation at the [5,6] bond, lies 0.78 eV higher than isomer A. In short, the product will be dominated by isomers A and B.

Figure 6 shows the three isomers of $C_{48}N_{12}H_2$ considered in this work. The energy of hydrogenation (=−1.55 eV) for the most stable isomer (=isomer E_{5C-6C}) indicates that $C_{48}N_{12}$ can be hydrogenated slightly more easily than C_{60}. It is characterized by the hydrogenation at the [5,6] bond in the equatorial region;

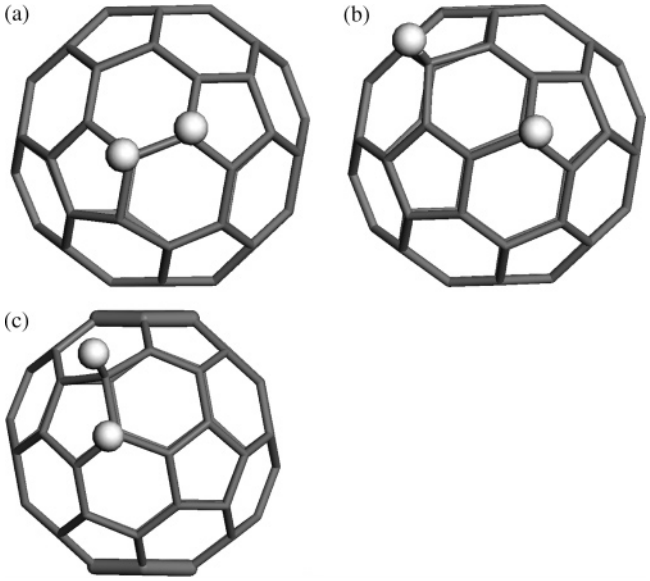

Figure 5. Optimized structures of isomers A (a), B (b), and C (c) of $C_{60}H_2$.

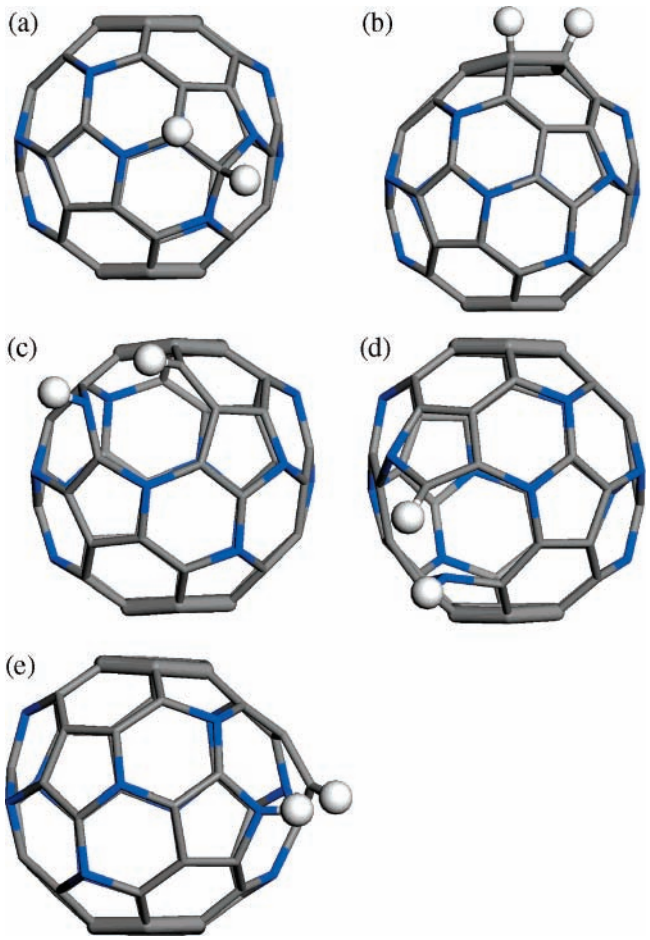

Figure 6. Optimized structures of the isomers of $C_{48}N_{12}H_2$: E_{5C-6C} (a), P_{6C-6C} (b), B_{5C-6N} (c), E_{5C-6N} (d), and E_{6C-6N} (e). Also refer to the caption of Figure 2.

however, the hydrogenation at other sites is much less feasible, and the product will be solely dominated by isomer E_{5C-6C}. Namely, isomer P_{6C-6C}, which corresponds to the hydrogenation at the [6,6] bond in the polar region, is much less (by 1.42 eV) stable. Isomer B_{5C-6N}, which corresponds to hydrogenation at the [5,6] C−N bond, is even less stable.

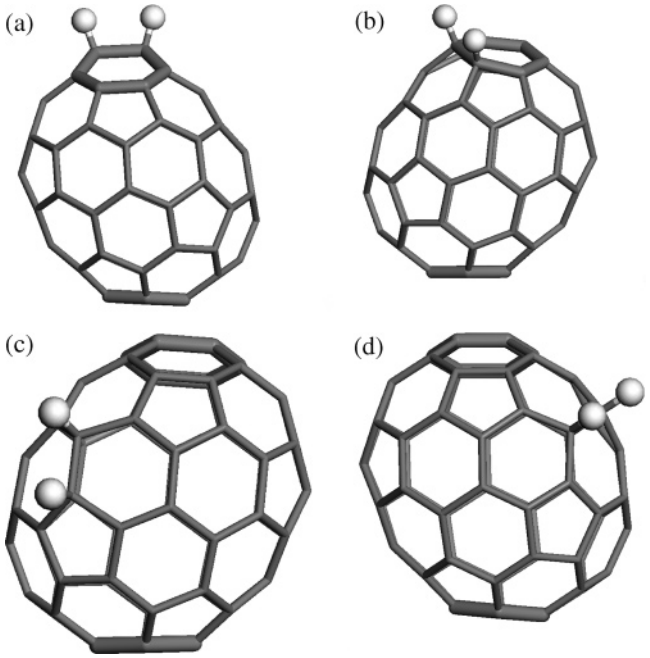

Figure 7. Optimized structures for isomers of $C_{70}H_2$: $P_{6C-6C}{}^{\alpha}$ (a), $P_{6C-6C}{}^{\beta}$ (b), $E_{6C-6C}{}^{\delta}$ (c), and $E_{6C-6C}{}^{\eta}$ (d). Superscripts (=α, β, δ, and η) represent the positions shown in Figure 8. Also refer to the caption of Figure 2.

We also investigated the hydrogenation of C_{70}. According to the fullerene reactivity principle, the [6,6] bonds in the polar regions of C_{70} are more reactive than others due to the local curvature of the region.[26] Our calculations matched these results. In Table 4, the energy of hydrogenation (=−0.84 eV) for the most stable isomer (=isomer $P_{6C-6C}{}^{\alpha}$) indicates that the hydrogenation tendency of C_{70} is similar to that of C_{60}. Figure 7a shows that it is characterized by hydrogenation at a [6,6]α bond in the polar region, where α designates the position shown in Figure 8a. The table also shows that isomer $P_{6C-6C}{}^{\beta}$, which can be described by the hydrogenation at the polar [6,6]β bond, is almost as favorable. As indicated in the table, hydrogenations at equatorial positions are much less favorable, and the hydrogenation product will be dominated by isomers $P_{6C-6C}{}^{\alpha}$ and $P_{6C-6C}{}^{\beta}$. When compared with the case for oxygenation described above, the hydrogenation of C_{70} occurs in a more regiospecific way; i.e., the reaction occurs predominantly in the polar region.

Now, we investigate the hydrogenation of $C_{58}N_{12}$. The energy (=−0.60 eV) of the reaction for the most stable isomer (=isomer $E_{5C-6C}{}^{\zeta}$) in Table 4 indicates that the molecules are slightly less easily subject to hydrogenation than $C_{48}N_{12}$. Figures 9 and S3 (Supporting Information) show that the isomer is characterized by H_2-addition to the [5,6]ζ C=C bond in the equatorial region. Other isomers are at least 0.46 eV less stable. They also include isomers $E_{6C-6C}{}^{\delta}$ and $P_{6C-6C}{}^{\alpha}$ shown in Figures 9b and S3a (Supporting Information), in which hydrogenation involves the [6,6]δ and the [6,6]α C=C bonds, respectively. In short, the product will be dominated by isomer $E_{5C-6C}{}^{\zeta}$ in which hydrogenation occurs in the equatorial region, not in the polar region. We can easily find that this is in strong contrast with the case of C_{70}, thereby revealing the change of regiospecificity upon N-substitution.

Here, we discuss the encapsulation of a nitrogen atom in the N-doped fullerenes in comparison with those which are undoped.

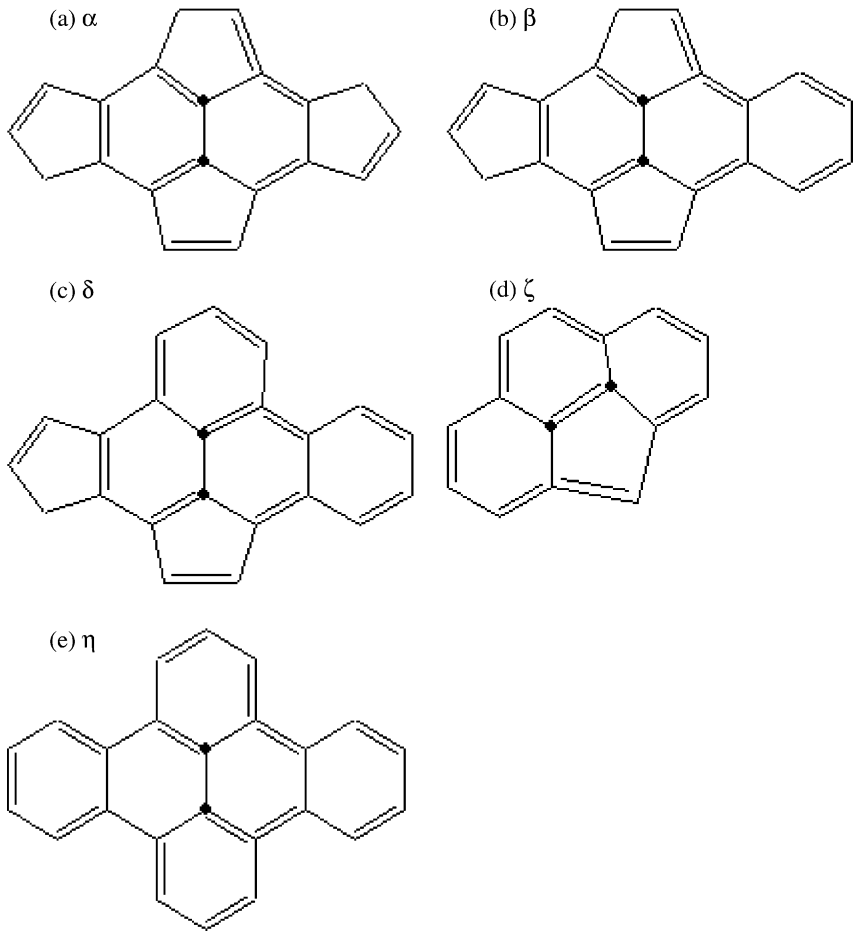

Figure 8. Five possible bond types for hydrogenation, α (a), β (b), δ (c), ζ (d), and η (e) in C_{70} and $C_{58}N_{12}$.

TABLE 5: Various Parameters for the Stable Isomers of $N@C_{60}$, $N@C_{48}N_{12}$, $N@C_{70}$, and $N@C_{58}N_{12}$

	isomer[a]	ΔE (eV)	multiplicity	$l(N_{en}-Ci)$[b]	$l(C1-C2)$[c]	WBI($N_{en}-Ci$)[d]	NBO charge[e]
$N@C_{60}$	C	0.03	4				0
$N@C_{48}N_{12}$	E_{5C-6C}	-1.03	2	1.50, 1.48	1.43 (1.37)	0.91, 0.94	−0.40
	C	-0.09	4				−0.09
$N@C_{70}$	C	0.01	4				0
$N@C_{58}N_{12}$	E_{6C-6C}	-3.20	2	1.41, 1.41	1.42 (1.37)	1.13, 1.13	−0.62
	E_{5C-6C}	-1.20	2	1.47, 1.41	1.41 (1.38)	0.96, 1.09	−0.61
	$E_{6C-6C'}$	-0.77	2	1.53, 1.41	1.46 (1.43)	0.82, 1.05	−0.50
	C	-0.26	4	2.59, 2.66	1.42 (1.42)	0.02, 0.01	−0.19
	$E_{5C-6C'}$	-0.23	2	1.51, 1.43	1.44 (1.41)	0.85, 1.00	−0.48

[a] Isomers are labeled according to the type of C−C bond at which N_{en} binds. Isomer "C" denotes that N_{en} is located at or near the center of the cage. [b] Bond distances for $N_{en}-C1$ and $N_{en}-C2$, where C1 and C2 denote carbon atoms of the C−C bond indicated by the isomer's name. [c] C1−C2 bond distance. Numbers in parentheses denote the corresponding values before N-encapsulation. [d] Wiberg bond indices for the bonds $N_{en}-C1$ and $N_{en}-C2$. [e] Charge of the atom N_{en} obtained from the natural bond orbital (NBO) analysis.

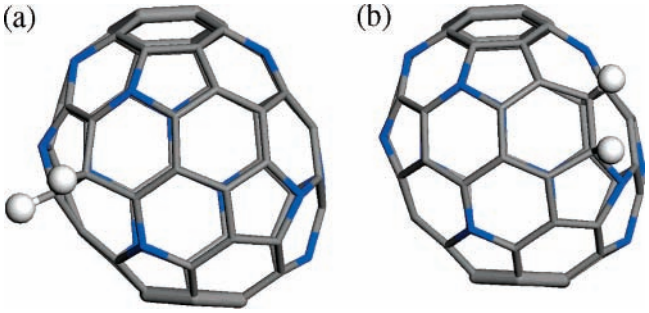

Figure 9. Optimized structures of isomers of $C_{58}N_{12}H_2$: $E_{5C-6C}{}^{\xi}$ (a) and $E_{6C-6C}{}^{\delta}$ (b). Also refer to the caption of Figure 2.

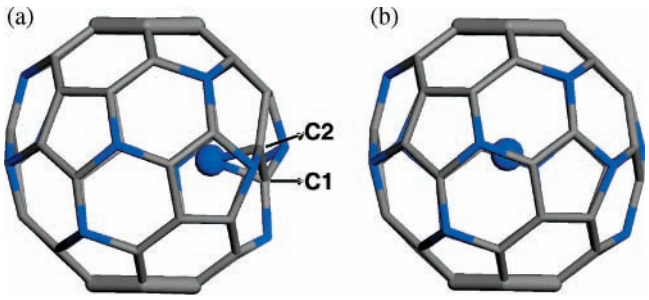

Figure 10. Optimized structures of the isomers of $N@C_{48}N_{12}$: E_{5C-6C} (a) and C (b). Also refer to the caption of Figure 2.

To do this, we define the encapsulation energy [$=\Delta E_{en}$(fullerene)] by the relation N_{en} + fullerene → N_{en}@fullerene, where N_{en} is the encapsulated atom. We first considered $C_{48}N_{12}$. The six isomers were identified which are different from one another in which the atom N_{en} is located at different positions in the cage, while Table 5 shows that two of the isomers are the most stable. We find that the nitrogen atom can be encased in $C_{48}N_{12}$ better than in C_{60}, as indicated by the negative values (=−1.03 and −0.09 eV) of $\Delta E_{en}(C_{48}N_{12})$. [For comparison, we note that $\Delta E_{en}(C_{60}) = 0.03$ eV, and $N@C_{60}$ were experimentally identified. Four other isomers of $N@C_{48}N_{12}$ not listed in the table have positive values of $\Delta E_{en}(C_{48}N_{12})$.] In the most stable isomer (=E_{5C-6C}) shown in Figure 10a, N_{en} is bonded with two [5,6] carbon atoms (=C1 and C2) in the equatorial region of the cage. [This is clearly different from the case of the nitrogen encapsulation in C_{60}, where N_{en} is located at the center of the cage without losing its atomic character. In fact, Figure 10b shows that N_{en} is located at the central position in the next stable isomer (=isomer C) of $N@C_{48}N_{12}$, and Table 5 shows that it is less stable by 0.94 eV.] In fact, the bond lengths (=1.50 and 1.48 Å) for $N_{en}-C1$ and $N_{en}-C2$ bonds in isomer E_{5C-6C} indicate that they are single bonds. As a result, the bond length (=1.43 Å) between atoms C1 and C2 becomes longer after the

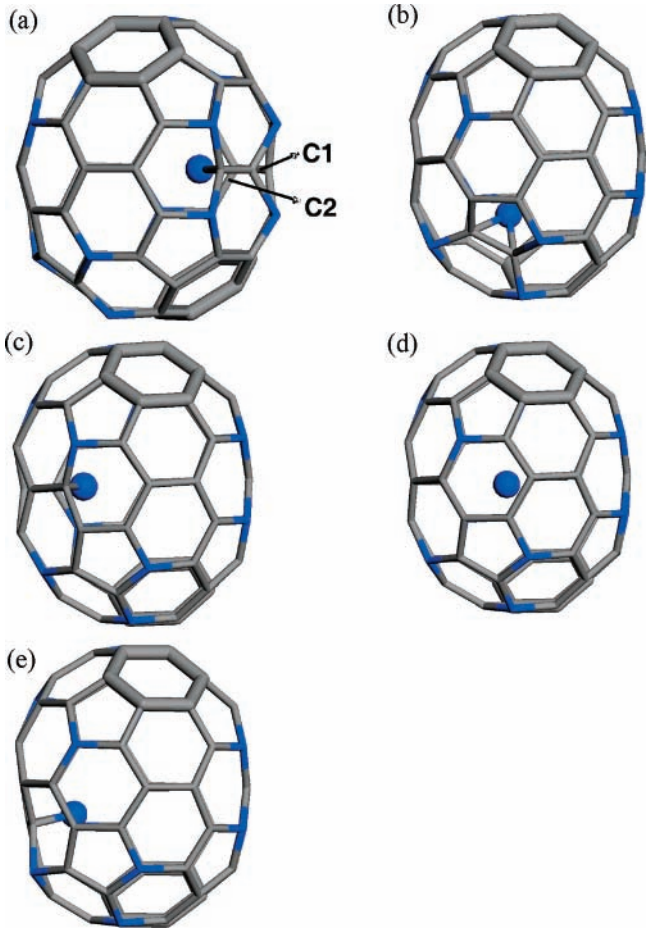

Figure 11. Optimized structures for the isomers of $N@C_{58}N_{12}$: E_{6C-6C} (a), E_{5C-6C} (b), $E_{6C-6C'}$ (c), C (d), and $E_{5C-6C'}$ (e).

encapsulation. Our separate analysis shows that the Wiberg bond index[27] (WBI) of the bond calculated with the GAUSSIAN03[28] program changes from 1.51 to 0.96 after the encapsulation of N_{en}, showing that the C1−C2 bond becomes a single bond. C1 and C2 subside in the tube by approximately 0.38 Å after the N-encapsulation in order to achieve a sp^3 hybridization. Another calculation shows that the spin density is concentrated on N_{en}. All these observations are consistent with the spin multiplicity (=doublet) of the system that is different from that (=quartet) of $N@C_{60}$.

Here, we delve into the N-encapsulation of $C_{58}N_{12}$. Table 5 shows the various parameters for the stable isomers considered in this work, which have the encapsulation energies larger than that of $N@C_{70}$. Figure 11 shows their structures. [Although not explained, we have also found two other isomers whose ΔE_{en}-

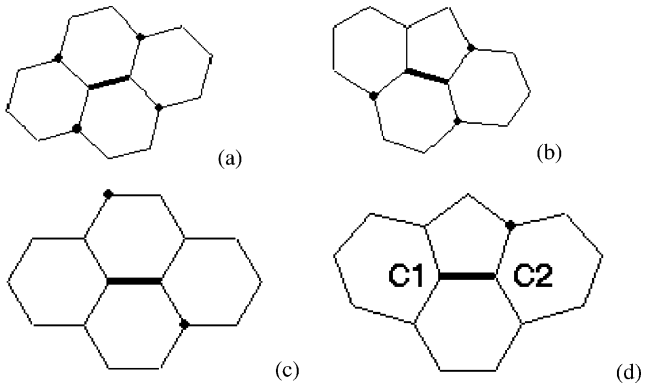

Figure 12. Local environments for the cage of $C_{58}N_{12}$ around N_{en} for the isomers E_{6C-6C} (a), E_{5C-6C} (b), $E_{6C-6C'}$ (c), and $E_{5C-6C'}$ (d). The thick lines indicate C−C bonds whose atoms are involved in the formation of N_{en}−C bonds. The dots represent the nitrogen atoms substitutionally doped in $C_{58}N_{12}$.

($C_{58}N_{12}$) are positive.] The most stable isomer (=E_{6C-6C}) is characterized by the single bonds for N_{en}−C1 and N_{en}−C2 pairs, where C1 and C2 belong to the [6,6] bond located at the equatorial region of the cage. [See Figure 12a.] [It is worth noting that different C−C bonds are involved in the formation of N_{en}−C bonds for the most stable isomer of $N@C_{48}N_{12}$ and $N@C_{58}N_{12}$.] Its N-encapsulation energy (=−3.20 eV) indicates that it is much easier to encase an N atom in $C_{58}N_{12}$ than in C_{60}, C_{70}, or even $C_{48}N_{12}$. In fact, the bond lengths and WBI for N_{en}−C1 and N_{en}−C2 bonds are (1.41 Å, 1.13) and (1.41 Å, 1,13), respectively, and thus the bonds are stronger than the corresponding ones in isomer E_{5C-6C} of $N@C_{48}N_{12}$. [Table 5 shows that the WBI for the corresponding bonds in the latter are 0.94 and 0.91.] The C1−C2 bond (=1.42 Å) gets elongated as a result of the N-encapsulation. C1 and C2 subside in the tube by ∼0.35 Å. All these observations are also consistent with the spin configuration (=doublet) of the system.

The next stable isomer, E_{5C-6C}, is characterized by the two N_{en}−C bonds involving the two carbon atoms (=C1 and C2) of the [5,6] bond in the equatorial region. [See Figure 12b.] One of the N_{en}−C bond lengths (=1.47 Å) is longer than the corresponding one in the most stable isomer, which should correlate with a smaller encapsulation energy (=−1.20 eV). C1 and C2 also subside in the cage by 0.47 Å upon the N-encapsulation. The third isomer, $E_{6C-6C'}$, also has the N_{en}−C bonds involving a carbon atom in the [6,6] bond. This isomer, however, is different from the most stable isomer in that its substitutional nitrogen atoms are distributed differently around the [6,6] bond. [Compare Figure 12c with Figure 12a.] One of the N_{en}−C bonds is still weaker, as manifested in (the bond length, WBI) = (1.53 Å, 0.82). C1 and C2 also subside in the tube. The negative value of $\Delta E_{en}(C_{58}N_{12})$ [=−0.26 eV] for isomer C seems to be related to the fact that N_{en} is displaced from the center of the cage toward the short axis of the cage by ∼1.0 Å, whereas, there are still no N_{en}−C bonds, as shown in the distances (=2.59 and 2.66 Å) from N_{en} to the nearest pair of carbon atoms. [See Table 5.] This is consistent with the fact that the spin multiplicity of the isomer is quartet. Comparison of its $\Delta E_{en}(C_{58}N_{12})$ and those of the more stable ones suggests that the atom N_{en} is presumably bonded to carbon atoms of the cage rather than being located at the center with no N_{en}−C bonds. The least stable isomer among the four shown in Figure 11e is characterized by the smallest number of the adjacent nitrogen atoms, as indicated in Figure 12e. Inversely, the most stable isomer, E_{6C-6C}, has the maximum (=4) number of substitutional nitrogen atoms around the [6,6] bond involved in the bond formation with N_{en}. Compared to the case of the least stable isomer, $E_{5C-6C'}$, C1 and C2 are much more positively charged in E_{6C-6C}, since the substitutional nitrogen atoms strongly withdraw electrons from the atoms of the [6,6] bond. In turn, this makes N_{en}−C1 and N_{en}−C2 bonds much stronger due to the stronger electrostatic attraction between N_{en} and C1 as well as between N_{en} and C2. This is indirectly manifested in the differentiation of the bond lengths for N_{en}−C1 and N_{en}−C2. For example, the corresponding data are 1.51 and 1.43 Å in the isomer $E_{5C-6C'}$. [See Figure 12d for the definition of C1 and C2.] Namely, the latter is shorter because C2 is more positively charged than C1. In short, substitutional nitrogen atoms induce a strong binding between the adjacent carbon atom and N_{en}.

4. Conclusion

First, we find that $C_{58}N_{12}$ can be the stable N-dopant of C_{70} just as $C_{48}N_{12}$ is that of C_{60}. By considering many different isomers of the product, we find that $C_{48}N_{12}$ is expected to be more easily subject to oxygenation than C_{60}. Meanwhile, similar calculations show that $C_{58}N_{12}$ is as stable as C_{70} with respect to oxygenation; however, $C_{48}N_{12}O$ is only 0.51 eV less stable than C_{70} with respect to the reaction. Combining these observations with the fact that C_{70} is not easily oxygenated in the air under normal conditions,[23] we expect that both $C_{48}N_{12}$ and $C_{58}N_{12}$ would also be stable in the air with respect to oxygenation. For both $C_{48}N_{12}O$ and $C_{58}N_{12}O$, we have identified many stable isomers in which oxygenation occurs at the C−N bonds as well as at the C−C bonds, among which particular C−N bonds are expected to be the most amenable to the reaction. Hydrogenations of $C_{48}N_{12}$ and $C_{58}N_{12}$ were also investigated. We find that the former can be more easily hydrogenated than C_{60}, while the latter is not. In addition, there is a regiospecificity in the hydrogenated products of $C_{48}N_{12}$ and $C_{58}N_{12}$ in that they prefer to react at equatorial sites. Also, $C_{58}N_{12}$ is strongly different from C_{70} in the preferred hydrogenation site.

Finally, we have compared the relative ease of the encapsulation of the nitrogen atom in C_{60}, $C_{48}N_{12}$, C_{70}, and $C_{58}N_{12}$, finding that the N-doped fullerenes, especially $C_{58}N_{12}$, can do this much better than the undoped fullerenes. Considering that $N@C_{60}$ was experimentally identified, we can easily expect the existence of $N@C_{48}N_{12}$ and $N@C_{58}N_{12}$. Contrary to the case of $N@C_{60}$ and $N@C_{70}$, N_{en} in $N@C_{48}N_{12}$ or $N@C_{58}N_{12}$ is not located at the center of the cage but significantly displaced toward the wall of the cages so that N_{en}−C bonds can be formed. In addition, the relative stability of the complexes heavily depends on the local environment of the carbon atoms involved in N_{en}−C bonds. We expect that the present work would stimulate experimental investigations on the identification of $C_{58}N_{12}$, $N@C_{48}N_{12}$, and $N@C_{58}N_{12}$ as well as their applications in the nanoelectronic devices.

Acknowledgment. We would like to extend our thanks to Jeonju University for its financial support. We also would like to acknowledge the support from KISTI (Korea Institute of Science and Technology Information) under the 7th Strategic Supercomputing Applications Support Program. The use of the computing system of the Supercomputing Center is also greatly appreciated.

Supporting Information Available: Figures showing the optimized structures of isomers of $C_{48}N_{12}O$, $C_{58}N_{12}O$, and

$C_{58}N_{12}H_2$. This material is available free of charge via the Internet at http://pubs.acs.org.

References and Notes

(1) Brown, C. M.; Beer, E.; Bellavia, C.; Cristofolini, L.; Gonzalez, R.; Hanfland, M.; Hausermann, D.; Keshavarz-K, M.; Kordatos, K.; Prassides, K.; Wudl, F. *J. Am. Chem. Soc.* **1996**, *118*, 8715.

(2) Hultman, L.; Stafström, S.; Czigány, Z.; Neidhardt, J.; Hellgren, N.; Brunell, I. F.; Suenaga, K.; Colliex, C. *Phys. Rev. Lett.* **2001**, *87*, 225503.

(3) Xie, R. H.; Bryant, G. W.; Zhao, J.; Smith, V. H., Jr.; Di Carlo, A.; Pecchia, A. *Phys. Rev. Lett.* **2003**, *90*, 206602.

(4) Manaa, M. R.; Sprehn, D. W.; Ichord, H. A. *J. Am. Chem. Soc.* **2002**, *124*, 13990.

(5) Stafström, S.; Hultman, L.; Hellgre, N. *Chem. Phys. Lett.* **2001**, *340*, 227.

(6) Xie, R. H.; Bryant, G. W.; Jensen, L.; Zhao, J.; Smith, H. *J. Chem. Phys.* **2003**, *118*, 8621.

(7) Xie, R. H.; Bryant, G. W.; Smith, V. H. *Chem. Phys. Lett.* **2003**, *368*, 486.

(8) Xie, R. H.; Bryant, G. W.; Smith, V. H. *Phys. Rev. B* **2003**, *67*, 155404.

(9) Manaa, M. R. *Solid State Commun.* **2004**, *129*, 379.

(10) Delaney, P.; Greer, J. C. *Appl. Phys. Lett.* **2004**, *84*, 431.

(11) (a) Kresse, G.; Hafner, J. *Phys. Rev. B* **1993**, *47*, RC558. (b) Kresse, G.; Furthmuller, J. *Phys. Rev. B* **1996**, *54*, 11169.

(12) Kresse, G.; Joubert, D. *Phys. Rev. B* **1999**, *59*, 1758.

(13) Perdew, J. P.; Burke, K.; Ernzerhof, M. *Phys. Rev. Lett.* **1996**, *77*, 3865.

(14) (a) Kang, H. S. *J. Phys. Chem. A* **2005**, *109*, 478. (b) Kang, H. S. *J. Phys. Chem. A* **2005**, *109*, 1458. (c) Kang, H. S. *J. Phys. Chem. A* **2005**, *109*, 4342. (d) Kang, H. S. *J. Am. Chem. Soc.* **2005**, *127*, 9839. (e) Kang, H. S. *J. Phys. Chem. A* **2005**, *109*, 9292.

(15) Wood, J. M.; Kahr, B.; Hoke, S. H., II.; Dejarme, L.; Cooks, R. G.; Ben-Amotz, D. *J. Am. Chem. Soc.* **1991**, *113*, 5907.

(16) Creegan, K. M.; Robbins, J. L.; Robbins, W. K.; Millar, J. M.; Sherwood, R. D.; Tindall, P. J.; Cox, D. M.; Smith, A. B., III; McCauley, J. P.; Jones, D. R.; Gallagher, R. T. *J. Am. Chem. Soc.* **1992**, *114*, 1103.

(17) (a) Elemes, Y.; Silverman, S. K.; Sheu, C.; Kao, M.; Foote, C. S.; Alvarez, M. M.; Whetten, R. L. *Angew. Chem.* **1992**, *104*, 364. (b) Elemes, Y.; Silverman, S. K.; Sheu, C.; Kao, M.; Foote, C. S.; Alvarez, M. M.; Whetten, R. L. *Angew. Chem., Int. Ed. Engl.* **1992**, *31*, 351.

(18) Weisman, R. B.; Heymann, D.; Bachilo, S. M. *J. Am. Chem. Soc.* **2001**, *123*, 9720.

(19) Raghavachari, K. *Chem. Phys. Lett.* **1992**, *195*, 221.

(20) Raghavachari, K.; Sosa, C. *Chem. Phys. Lett.* **1993**, *209*, 223.

(21) *Inorganic Chemistry: Principles of Structure and Reactivity*, 4th ed.; Huheey, J. E., Keiter, E. A., Keiter, R. L., Eds.; HarperCollins College Publishers: New York, 1993; p A-33.

(22) Raghavachari, K.; Rohlfing, C. M. *Chem. Phys. Lett.* **1992**, *197*, 495.

(23) Diederich, F.; Ettl, R.; Rubin, Y.; Whetten, R. L.; Beck, R.; Alvarez, M.; Anz, S.; Sehsharma, D.; Wudl, F.; Khemani, K. C.; Koch, A. *Science* **1991**, *252*, 548.

(24) Heymann, D.; Bachilo, S. M.; Weisman, R. B. *J. Am. Chem. Soc.* **2002**, *124*, 6317.

(25) Bühl, M.; Hirsch, A. *Chem. Rev.* **2001**, *101*, 1153.

(26) (a) Thilgen, C.; Herrmann, A.; Diederich, F. *Angew. Chem.* **1997**, *109*, 2362. (b) Thilgen, C.; Herrmann, A.; Diederich, F. *Angew. Chem., Int. Ed. Engl.* **1997**, *36*, 2269.

(27) (a) Reed, A. E.; Weinstock, R. B.; Weinhold, F. *J. Chem. Phys.* **1985**, *83*, 735. (b) Reed. A. E.; Weinhold, F. *Chem. Rev.* **1988**, *88*, 899. (c) Reed, A. E.; Schleyer, P. v. R. *J. Am. Chem. Soc.* **1990**, *112*, 1434.

(28) Frisch, M. J.; Trucks, G. W.; Schlegel, H. B.; Scuseria, G. E.; Robb, M. A.; Cheeseman, J. R.; Montgomery, J. A., Jr.; Vreven, T.; Kudin, K. N.; Burant, J. C.; Millam, J. M.; Iyengar, S. S.; Tomasi, J.; Barone, V.; Mennucci, B.; Cossi, M.; Scalmani, G.; Rega, N.; Petersson, G. A.; Nakatsuji, H.; Hada, M.; Ehara, M.; Toyota, K.; Fukuda, R.; Hasegawa, J.; Ishida, M.; Nakajima, T.; Honda, Y.; Kitao, O.; Nakai, H.; Klene, M.; Li, X.; Knox, J. E.; Hratchian, H. P.; Cross, J. B.; Adamo, C.; Jaramillo, J.; Gomperts, R.; Stratmann, R. E.; Yazyev, O.; Austin, A. J.; Cammi, R.; Pomelli, C.; Ochterski, J. W.; Ayala, P. Y.; Morokuma, K.; Voth, G. A.; Salvador, P.; Dannenberg, J. J.; Zakrzewski, V. G.; Dapprich, S.; Daniels, A. D.; Strain, M. C.; Farkas, O.; Malick, D. K.; Rabuck, A. D.; Raghavachari, K.; Foresman, J. B.; Ortiz, J. V.; Cui, Q.; Baboul, A. G.; Clifford, S.; Cioslowski, J.; Stefanov, B. B.; Liu, G.; Liashenko, A.; Piskorz, P.; Komaromi, I.; Martin, R. L.; Fox, D. J.; Keith, T.; Al-Laham, M. A.; Peng, C. Y.; Nanayakkara, A.; Challacombe, M.; Gill, P. M. W.; Johnson, B.; Chen, W.; Wong, M. W.; Gonzalez, C.; Pople, J. A. *Gaussian03*, Revision B.05; Gaussian, Inc.: Pittsburgh, PA, 2003.

(29) Reed, A. E.; Curtiss, L. E.; Weinhold, F. *Chem. Rev.* **1988**, *88*, 899.